JOURNAL OF GUIDANCE, CONTROL, AND DYNAMICS
Vol. 17, No. 5, September–October 1994

Substructure System Identification and Synthesis

Tzu-Jeng Su* and Jer-Nan Juang†
NASA Langley Research Center, Hampton, Virginia 23681

This paper explores the possibility of performing system identification at the substructure level and then synthesizing the results to obtain an analysis model for the assembled structure. The study here shows that to produce exact substructure coupling, the input–output transfer function relations among all of the interface degrees of freedom must be measured. Procedures for assembling substructure transfer function data, substructure state-space models, and substructure Markov parameters are presented. Some potential testing difficulties and possible solution approaches are also discussed. A mass-loaded interface approach is proposed to produce interface excitations without using actuators. A spring-supported boundary approach is developed for the testing of free substructures. Some feasible testing setups for the measurement and excitation of the interface rotational degrees of freedom are also included. The proposed methods are illustrated by a numerical example.

Introduction

ALTHOUGH the finite element method has been used widely as a powerful tool for deriving analysis models for flexible structures, at times structural and control engineers prefer using an experimental approach, because the models derived from test data are usually more accurate than the finite-element models. However, when the structure is large and has densely clustered frequencies, it can be difficult to perform experiments as well as to derive an accurate model from the test data. In this case, a substructure-based approach will prove to be useful.

Most research work on substructure-based testing and analysis has been related to the component mode synthesis (CMS) method, of which an excellent review can be found in Ref. 1. In the CMS method, substructure models are represented in a second-order form by using a set of modes including normal modes and/or static modes as the modeling basis. Then, synthesis of substructure models is done by enforcing compatibility and equilibrium conditions along the interfaces between substructures. Although the CMS method has been used in combination with the modal testing and modal analysis techniques[2,3] in substructure experiments, it has many limitations and disadvantages. First, measuring the mode shapes of a substructure requires placing sensors all over the surface of the substructure, which usually is not practical. Second, there exists no effective method so far for measuring the static mode shapes. Without the static modes, a large number of the substructures' normal modes must be measured and included to obtain accurate substructure models. Third, most modal analysis methods neglect damping or assume it to be proportional, which in general cannot closely describe the system's actual damping behavior.

Other than the modal testing/modal analysis approach, there are many system identification methods that also can be used to identify an analysis model from the test data, e.g., the methods in Refs. 4 and 5. A system identification approach does not require measurement of mode shapes and makes no assumption on the damping. The only test data needed for system identification are the input and output time history data or frequency response data. The system identification results are usually presented in an input–output transfer function expression or in the first-order state-space form, which covers a much wider class of linear systems than the second-order modal models and, hence, can match the test data more closely. There are many advantages of using a system identification approach to identify structure models. However, to the authors' knowledge, there is no existing literature related to substructure-based system identification. The main purpose of this paper is to explore the possibility of using a system identification approach to perform substructure synthesis.

It is found that substructure-based system identification can follow either of the two procedures shown in Fig. 1. Briefly speaking, one can either choose to synthesize substructure test data first and then carry out system identification at the global level based on the assembled test data or choose to perform system identification at the substructure level first and then employ substructure synthesis to assemble substructure models. Although both approaches are theoretically feasible, it is preferred to perform system identification at the substructure level, mainly because substructures are easier to identify than the assembled structure.

System identification can be done in the frequency domain by using transfer function data or in the time domain by using pulse response data or Markov parameters (see Ref. 6). One contribution of this paper is the development of the synthesis procedures for assembling substructure transfer functions, substructure state-space models, and substructure Markov parameters. It is shown that in order to enforce interface compatibility and equilibrium conditions by using substructure input and output test data, there must be collocated actuators and sensors at all of the interface degrees of freedom. Another contribution of this paper is the discussion of potential testing difficulties and possible solution approaches. A mass-loaded interface approach is proposed to produce interface excitations without using actuators. A spring-supported boundary approach is developed for the testing and system identification of free substructures. Discussions also include the measurement and excitation of the interface rotational degrees of freedom and the effect of discrete-time data sampling to the accuracy of substructure synthesis.

This paper is organized as follows. First, the procedures for assembling substructure transfer functions, substructure state-space models, and substructure Markov parameters are developed separately. Then, some testing difficulties are discussed along with possible solution approaches proposed. A numerical example is included for illustration of the proposed methods. Finally, this paper is concluded with a few remarks.

Synthesis of Substructure Transfer Functions

First, the procedure for assembling substructure transfer functions of a two-substructure structure will be developed. Then, a general, systematic procedure for assembling multisubstructure structures will be derived. These procedures can be used to assemble substructure transfer function data measured at a sequence of frequency points, or they can be used to assemble substructure transfer function models if the substructure system identification results are represented by transfer function expressions.

Received March 16, 1993; revision received Aug. 12,1993; accepted for publication Sept. 28, 1993.

*National Research Council Research Associate. Member AIAA.
†Principal Scientist, Spacecraft Dynamics Branch. Fellow AIAA.

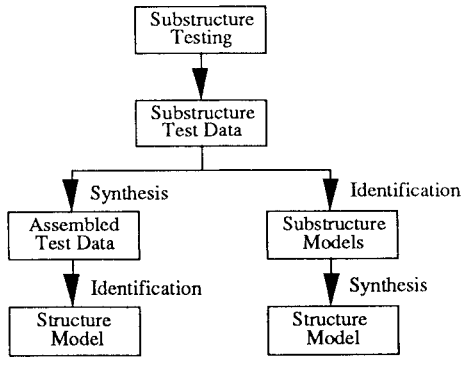

Fig. 1 Substructure system identification and synthesis procedures.

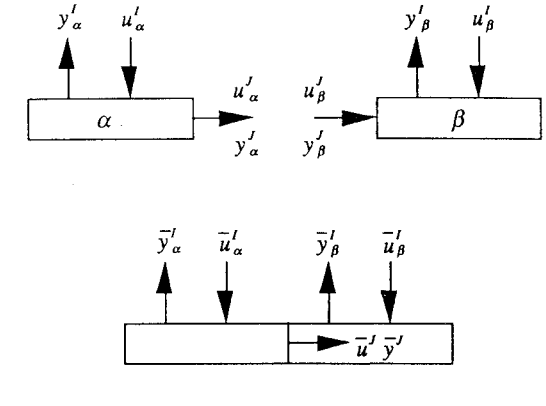

Fig. 2 A structure composed of two substructures.

Two-Substructure Case

A structure composed of two substructures is shown in Fig. 2. Figure 2a shows the two decoupled substructures α and β. Locations of actuators and sensors are denoted by u and y, respectively. The actuators and sensors of each substructure are divided into two groups. Those actuators and sensors located at the joint (or interface, where the substructures are to be connected together) are denoted with a superscript J. Those actuators and sensors located at the unconnected points (or interior points) of the substructures are denoted with a superscript I. To describe interface compatibility and equilibrium conditions in terms of input and output vectors, it is assumed that each substructure is allocated an actuator/sensor pair at every interface degree of freedom. The type of sensors placed at the interface can be a displacement sensor, a velocity sensor, or an accelerometer. The actuators placed at the interface must be able to produce force-type inputs. The actuators and sensors located at the interior points can be of any type and do not have to be collocated. Figure 2b shows the assembled structure. Throughout this paper, all the variables and quantities of the assembled structure will be designated with an overbar, i.e., $\bar{(\ )}$.

Assume that the two substructures are tested separately with their interface degrees of freedom free of any constraint, that is, free-interface testing. Let the substructure testing results be represented in the frequency domain by the following two input–output transfer function relations:

$$\begin{Bmatrix} Y_\alpha^I \\ Y_\alpha^J \end{Bmatrix} = \begin{bmatrix} H_\alpha^{II} & H_\alpha^{IJ} \\ H_\alpha^{JI} & H_\alpha^{JJ} \end{bmatrix} \begin{Bmatrix} U_\alpha^I \\ U_\alpha^J \end{Bmatrix} \tag{1}$$

$$\begin{Bmatrix} Y_\beta^I \\ Y_\beta^J \end{Bmatrix} = \begin{bmatrix} H_\beta^{II} & H_\beta^{IJ} \\ H_\beta^{JI} & H_\beta^{JJ} \end{bmatrix} \begin{Bmatrix} U_\beta^I \\ U_\beta^J \end{Bmatrix} \tag{2}$$

All the quantities in the preceding two equations are functions of frequency, i.e., $Y_\alpha^I = Y_\alpha^I(j\omega)$, $H_\alpha^{II} = H_\alpha^{II}(j\omega)$, etc. Also, H_α^{IJ} denotes the transfer function matrix of the α-substructure from U_α^J to Y_α^I, and so forth. Similarly, let the global transfer function relation for the assembled structure be described by

$$\begin{Bmatrix} \bar{Y}_\alpha^I \\ \bar{Y}_\beta^I \\ \bar{Y}^J \end{Bmatrix} = \begin{bmatrix} \bar{H}_{11} & \bar{H}_{12} & \bar{H}_{13} \\ \bar{H}_{21} & \bar{H}_{22} & \bar{H}_{23} \\ \bar{H}_{31} & \bar{H}_{32} & \bar{H}_{33} \end{bmatrix} \begin{Bmatrix} \bar{U}_\alpha^I \\ \bar{U}_\beta^I \\ \bar{U}^J \end{Bmatrix} \tag{3}$$

The objective of substructure synthesis is to determine the global transfer function matrix from the measured substructure transfer function data. This objective can be achieved by using two interface conditions: compatibility and equilibrium. The output vectors at the interface are constrained by the compatibility equation:

$$\bar{Y}^J = Y_\alpha^J = Y_\beta^J \tag{4}$$

which says that the physical motion of the two substructures at the interface must be the same. The input vectors at the interface are related by the equilibrium equation:

$$\bar{U}^J = U_\alpha^J + U_\beta^J \tag{5}$$

which says that the sum of the internal forces at the interface must be equal to the external force applied there. By using Eq. (4), the bottom parts of Eqs. (1) and (2) can be rewritten as

$$U_\alpha^J = \left(H_\alpha^{JJ}\right)^{-1}\bar{Y}^J - \left(H_\alpha^{JJ}\right)^{-1}H_\alpha^{JI}U_\alpha^I \tag{6}$$

$$U_\beta^J = \left(H_\beta^{JJ}\right)^{-1}\bar{Y}^J - \left(H_\beta^{JJ}\right)^{-1}H_\beta^{JI}U_\beta^I \tag{7}$$

Then, by adding the preceding two equations and using Eq. (5), we obtain

$$\bar{Y}^J = \left[\left(H_\alpha^{JJ}\right)^{-1} + \left(H_\beta^{JJ}\right)^{-1}\right]^{-1}\left[\left(H_\alpha^{JJ}\right)^{-1}H_\alpha^{JI}U_\alpha^I + \left(H_\beta^{JJ}\right)^{-1}H_\beta^{JI}U_\beta^I + \bar{U}^J\right] \tag{8}$$

Finally, substituting Eqs. (6–8) and the following identities

$$Y_\alpha^I = \bar{Y}_\alpha^I, \qquad Y_\beta^I = \bar{Y}_\beta^I, \qquad U_\alpha^I = \bar{U}_\alpha^I, \qquad U_\beta^I = \bar{U}_\beta^I \tag{9}$$

into Eqs. (1) and (2), we obtain transfer function relations between the input and output vectors of the assembled structure. The results are

$$\begin{aligned}
\bar{H}_{11} &= H_\alpha^{II} - H_\alpha^{IJ}\left(H_\alpha^{JJ} + H_\beta^{JJ}\right)^{-1}H_\alpha^{JI} \\
\bar{H}_{12} &= H_\alpha^{IJ}\left(H_\alpha^{JJ} + H_\beta^{JJ}\right)^{-1}H_\beta^{JI} \\
\bar{H}_{13} &= H_\alpha^{IJ}\left(H_\alpha^{JJ} + H_\beta^{JJ}\right)^{-1}H_\beta^{JJ} \\
\bar{H}_{21} &= H_\beta^{IJ}\left(H_\alpha^{JJ} + H_\beta^{JJ}\right)^{-1}H_\alpha^{JI} \\
\bar{H}_{22} &= H_\beta^{II} - H_\beta^{IJ}\left(H_\alpha^{JJ} + H_\beta^{JJ}\right)^{-1}H_\beta^{JI} \\
\bar{H}_{23} &= H_\beta^{IJ}\left(H_\alpha^{JJ} + H_\beta^{JJ}\right)^{-1}H_\alpha^{JJ} \\
\bar{H}_{31} &= H_\beta^{JJ}\left(H_\alpha^{JJ} + H_\beta^{JJ}\right)^{-1}H_\alpha^{JI} \\
\bar{H}_{32} &= H_\alpha^{JJ}\left(H_\alpha^{JJ} + H_\beta^{JJ}\right)^{-1}H_\beta^{JI} \\
\bar{H}_{33} &= H_\alpha^{JJ}\left(H_\alpha^{JJ} + H_\beta^{JJ}\right)^{-1}H_\beta^{JJ}
\end{aligned} \tag{10}$$

The given transfer function expressions are the same as those derived in Ref. 7 by using the Lagrange multipliers method. These transfer function synthesis formulas also were used in Ref. 8 in model modification and optimal control of space structures.

Equation (10) shows that H_α^{JJ} and H_β^{JJ}, the substructure transfer functions from interface inputs to interface outputs, are the necessary data for performing substructure synthesis. Measuring these data requires placing collocated actuator/sensor pair at every interface degree of freedom. Later, in the discussion of testing difficulties we will propose using a mass-loaded interface approach to avoid this requirement.

Multiple-Substructure Case

For structures that are composed of more than two substructures, there is a systematic procedure to assemble substructure transfer functions. Let the input–output transfer function relation for the collection of the uncoupled substructures be represented by

$$\begin{Bmatrix} \mathbf{Y}^I \\ \mathbf{Y}^J \end{Bmatrix} = \begin{bmatrix} \mathbf{H}^{II} & \mathbf{H}^{IJ} \\ \mathbf{H}^{JI} & \mathbf{H}^{JJ} \end{bmatrix} \begin{Bmatrix} \mathbf{U}^I \\ \mathbf{U}^J \end{Bmatrix} \tag{11}$$

where

$$\mathbf{U}^I = \begin{Bmatrix} U_\alpha^I \\ U_\beta^I \\ U_\gamma^I \\ \vdots \end{Bmatrix}, \qquad \mathbf{U}^J = \begin{Bmatrix} U_\alpha^J \\ U_\beta^J \\ U_\gamma^J \\ \vdots \end{Bmatrix}$$

$$\mathbf{Y}^I = \begin{Bmatrix} Y_\alpha^I \\ Y_\beta^I \\ Y_\gamma^I \\ \vdots \end{Bmatrix}, \qquad \mathbf{Y}^J = \begin{Bmatrix} Y_\alpha^J \\ Y_\beta^J \\ Y_\gamma^J \\ \vdots \end{Bmatrix}$$

As before, Greek subscripts denote substructures, and superscripts I and J denote interior and joint (or interface) inputs and outputs, respectively. Similarly, let the input–output transfer function relation for the assembled structure be represented by

$$\begin{Bmatrix} \bar{\mathbf{Y}}^I \\ \bar{\mathbf{Y}}^J \end{Bmatrix} = \begin{Bmatrix} \bar{\mathbf{H}}^{II} & \bar{\mathbf{H}}^{IJ} \\ \bar{\mathbf{H}}^{JI} & \bar{\mathbf{H}}^{JJ} \end{Bmatrix} \begin{Bmatrix} \bar{\mathbf{U}}^I \\ \bar{\mathbf{U}}^J \end{Bmatrix} \tag{12}$$

Compatibility and equilibrium conditions along the interfaces between substructures can be summarized by using a coupling matrix $\boldsymbol{T}$ as

$$\mathbf{Y}^J = \mathbf{T}^T \bar{\mathbf{Y}}^J \tag{13}$$

$$\bar{\mathbf{U}}^J = \mathbf{T}\mathbf{U}^J \tag{14}$$

The coupling matrix $\boldsymbol{T}$ relates the interface outputs of the uncoupled substructures to the interface outputs of the assembled structure. Normally, the elements of the $\boldsymbol{T}$ matrix are ones and zeros. For example, for the two-substructure structure shown in Fig. 2, the coupling matrix is given by $\boldsymbol{T} = [I \quad I]$, where the identity matrix I has a dimension equal to the number of interface degrees of freedom.

By using the two conditions in Eqs. (13) and (14), the transfer functions of the assembled structure can be expressed in terms of the uncoupled substructure transfer functions. First, substitution of Eq. (13) into the bottom part of Eq. (11) gives

$$(\mathbf{H}^{JJ})^{-1}\mathbf{T}^T\bar{\mathbf{Y}}^J = (\mathbf{H}^{JJ})^{-1}\mathbf{H}^{JI}\mathbf{U}^I + \mathbf{U}^J \tag{15}$$

Premultiplying the preceding equation by $\boldsymbol{T}$ and using Eq. (14), we obtain

$$\bar{\mathbf{Y}}^J = \left[\mathbf{T}(\mathbf{H}^{JJ})^{-1}\mathbf{T}^T\right]^{-1}\left[\mathbf{T}(\mathbf{H}^{JJ})^{-1}\mathbf{H}^{JI}\mathbf{U}^I + \bar{\mathbf{U}}^J\right] \tag{16}$$

Finally, substitution of Eqs. (15) and (16) and the identities $\bar{\boldsymbol{U}}^I = \boldsymbol{U}^I$ and $\bar{\boldsymbol{Y}}^I = \boldsymbol{Y}^I$ into Eq. (11) yields the input–output transfer function relation for the assembled structure. The results are given by

$$\begin{aligned} \bar{\mathbf{H}}^{JJ} &= \left[\mathbf{T}(\mathbf{H}^{JJ})^{-1}\mathbf{T}^T\right]^{-1} \\ \bar{\mathbf{H}}^{II} &= \mathbf{H}^{II} - \mathbf{H}^{IJ}(\mathbf{H}^{JJ})^{-1}\mathbf{H}^{JI} \\ &\quad + \mathbf{H}^{IJ}(\mathbf{H}^{JJ})^{-1}\mathbf{T}^T\bar{\mathbf{H}}^{JJ}\mathbf{T}(\mathbf{H}^{JJ})^{-1}\mathbf{H}^{JI} \\ \bar{\mathbf{H}}^{IJ} &= \mathbf{H}^{IJ}(\mathbf{H}^{JJ})^{-1}\mathbf{T}^T\bar{\mathbf{H}}^{JJ} \\ \bar{\mathbf{H}}^{JI} &= \bar{\mathbf{H}}^{JJ}\boldsymbol{T}(\mathbf{H}^{JJ})^{-1}\mathbf{H}^{JI} \end{aligned} \tag{17}$$

Again, the necessary element for assembling substructures is the interface input–output transfer function $\boldsymbol{H}^{JJ}$.

Synthesis of Substructure State-Space Models

The assembling of substructure state-space models is also done by enforcing interface compatibility and equilibrium conditions. The first-order state-space models of substructures are represented by

$$\begin{aligned} \dot{x}_i &= A_i x_i + \begin{bmatrix} B_i^I & B_i^J \end{bmatrix} \begin{Bmatrix} u_i^I \\ u_i^J \end{Bmatrix} \\ \begin{Bmatrix} y_i^I \\ y_i^J \end{Bmatrix} &= \begin{bmatrix} C_i^I \\ C_i^J \end{bmatrix} x_i + \begin{bmatrix} D_i^{II} & D_i^{IJ} \\ D_i^{JI} & D_i^{JJ} \end{bmatrix} \begin{Bmatrix} u_i^I \\ u_i^J \end{Bmatrix} \end{aligned} \tag{18}$$

for $i = \alpha, \beta, \gamma, \ldots$. The preceding substructure state-space models are the results of system identification performed at the substructure level. The matrices A_i, B_i, C_i, and D_i represent the system matrix, the input influence matrix, the output influence matrix, and the direct force input term of the ith substructure, respectively. They are partitioned in accordance with the partitions of the input and output vectors. The vector x_i is the state vector of the ith substructure, which does not necessarily have physical meaning.

Define a system called the uncoupled-substructure system to be the system formed by the uncoupled substructures. A state-space model for the uncoupled-substructure system is described by

$$\begin{aligned} \dot{\mathbf{x}} &= \mathbf{A}_D\mathbf{x} + \begin{bmatrix} \mathbf{B}_D^I & \mathbf{B}_D^J \end{bmatrix} \begin{Bmatrix} \mathbf{u}^I \\ \mathbf{u}^J \end{Bmatrix} \\ \begin{Bmatrix} \mathbf{y}^I \\ \mathbf{y}^J \end{Bmatrix} &= \begin{bmatrix} \mathbf{C}_D^I \\ \mathbf{C}_D^J \end{bmatrix} \mathbf{x} + \begin{bmatrix} \mathbf{D}_D^{II} & \mathbf{D}_D^{IJ} \\ \mathbf{D}_D^{JI} & \mathbf{D}_D^{JJ} \end{bmatrix} \begin{Bmatrix} \mathbf{u}^I \\ \mathbf{u}^J \end{Bmatrix} \end{aligned} \tag{19}$$

where

$$\mathbf{u}^I = \begin{Bmatrix} u_\alpha^I \\ u_\beta^I \\ u_\gamma^I \\ \vdots \end{Bmatrix}, \qquad \mathbf{u}^J = \begin{Bmatrix} u_\alpha^J \\ u_\beta^J \\ u_\gamma^J \\ \vdots \end{Bmatrix}$$

$$\mathbf{y}^I = \begin{Bmatrix} y_\alpha^I \\ y_\beta^I \\ y_\gamma^I \\ \vdots \end{Bmatrix}, \qquad \mathbf{y}^J = \begin{Bmatrix} y_\alpha^J \\ y_\beta^J \\ y_\gamma^J \\ \vdots \end{Bmatrix}$$

And,

$$\mathbf{A} = \begin{bmatrix} A_\alpha & & & \\ & A_\beta & & \\ & & A_\gamma & \\ & & & \ddots \end{bmatrix}, \qquad \mathbf{B}_D^I = \begin{bmatrix} B_\alpha^I & & & \\ & B_\beta^I & & \\ & & B_\gamma^I & \\ & & & \ddots \end{bmatrix}, \ldots$$

$$\mathbf{C}_D^I = \begin{bmatrix} C_\alpha^I & & & \\ & C_\beta^I & & \\ & & C_\gamma^I & \\ & & & \ddots \end{bmatrix}, \qquad \mathbf{D}_D^{II} = \begin{bmatrix} D_\alpha^{II} & & & \\ & D_\beta^{II} & & \\ & & D_\gamma^{II} & \\ & & & \ddots \end{bmatrix}, \ldots \text{etc.}$$

are diagonal matrices. Define another system called the coupled-substructure system to be the system formed by the same collection of substructures but with compatibility and equilibrium conditions enforced at the interfaces between substructures. Let the state-space model of the coupled-substructure system be represented by

$$\begin{aligned} \dot{\mathbf{x}} &= \bar{\mathbf{A}}\mathbf{x} + [\bar{\mathbf{B}}^I \quad \bar{\mathbf{B}}^J] \begin{Bmatrix} \bar{\mathbf{u}}^I \\ \bar{\mathbf{u}}^J \end{Bmatrix} \\ \begin{Bmatrix} \bar{\mathbf{y}}^I \\ \bar{\mathbf{y}}^J \end{Bmatrix} &= \begin{bmatrix} \bar{\mathbf{C}}^I \\ \bar{\mathbf{C}}^J \end{bmatrix} \mathbf{x} + \begin{bmatrix} \bar{\mathbf{D}}^{II} & \bar{\mathbf{D}}^{IJ} \\ \bar{\mathbf{D}}^{JI} & \bar{\mathbf{D}}^{JJ} \end{bmatrix} \begin{Bmatrix} \bar{\mathbf{u}}^I \\ \bar{\mathbf{u}}^J \end{Bmatrix} \end{aligned} \tag{20}$$

Or, in short

$$\begin{aligned} \dot{\mathbf{x}} &= \bar{\mathbf{A}}\mathbf{x} + \bar{\mathbf{B}}\bar{\mathbf{u}} \\ \bar{\mathbf{y}} &= \bar{\mathbf{C}}\mathbf{x} + \bar{\mathbf{D}}\bar{\mathbf{u}} \end{aligned} \tag{21}$$

It should be mentioned that the coupled-substructure system is not the assembled structure. Note that whereas the coupled-substructure system has the same input and output vectors, $\bar{u}$ and $\bar{y}$, as the assembled structure, its state vector x is the same as that of the uncoupled-substructure system. Physically, the coupled-substructure system can be considered as obtained from connecting the substructures at the interfaces by using very short, massless, rigid links. The introduction of the coupled-substructure system is only for derivation purpose.

The interface inputs and outputs of the uncoupled-substructure system and the interface inputs and outputs of the coupled-substructure system are related by a coupling matrix T as

$$\mathbf{y}^J = \mathbf{T}^T \bar{\mathbf{y}}^J \tag{22}$$

$$\bar{\mathbf{u}}^J = \mathbf{T}\mathbf{u}^J \tag{23}$$

which essentially are the time-domain version of Eqs. (13) and (14). By substituting the compatibility condition $y^J = T^T \bar{y}^J$ and the identity $u^I = \bar{u}^I$ into the bottom part of the output equation in Eq. (19), we obtain

$$\mathbf{u}^J = \left(\mathbf{D}_D^{JJ}\right)^{-1}\left(\mathbf{T}^T\bar{\mathbf{y}}^J - \mathbf{C}_D^J\mathbf{x} - \mathbf{D}_D^{JI}\bar{\mathbf{u}}^I\right) \tag{24}$$

Premultiplication of the preceding equation by T and rearrangement yields

$$\bar{\mathbf{y}}^J = \left[\mathbf{T}\left(\mathbf{D}_D^{JJ}\right)^{-1}\mathbf{T}^T\right]^{-1}\left[\bar{\mathbf{u}}^J + \mathbf{T}\left(\mathbf{D}_D^{JJ}\right)^{-1}\mathbf{C}_D^J\mathbf{x} + \mathbf{T}\left(\mathbf{D}_D^{JJ}\right)^{-1}\mathbf{D}_D^{JI}\bar{\mathbf{u}}^I\right] \tag{25}$$

Finally, substituting Eqs. (24), (25), and the identities $u^I = \bar{u}^I$, $y^I = \bar{y}^I$ into Eq. (19), we obtain a state-space model for the coupled-substructure system. The results are

$$\begin{aligned}
\bar{\mathbf{A}} &= \mathbf{A}_D + \mathbf{B}_D^J\mathbf{Q}\mathbf{C}_D^J \\
\bar{\mathbf{B}} &= \begin{bmatrix} \mathbf{B}_D^I + \mathbf{B}_D^J\mathbf{Q}\mathbf{D}_D^{JI} & \mathbf{B}_D^J\left(\mathbf{D}_D^{JJ}\right)^{-1}\mathbf{T}^T\mathbf{S}^{-1} \end{bmatrix} \\
\bar{\mathbf{C}} &= \begin{bmatrix} \mathbf{C}_D^I + \mathbf{D}_D^{IJ}\mathbf{Q}\mathbf{C}_D^J \\ \mathbf{S}^{-1}\mathbf{T}\left(\mathbf{D}_D^{JJ}\right)^{-1}\mathbf{C}_D^J \end{bmatrix} \\
\bar{\mathbf{D}} &= \begin{bmatrix} \mathbf{D}_D^{II} + \mathbf{D}_D^{IJ}\mathbf{Q}\mathbf{D}_D^{JI} & \mathbf{D}_D^{IJ}\left(\mathbf{D}_D^{JJ}\right)^{-1}\mathbf{T}^T\mathbf{S}^{-1} \\ \mathbf{S}^{-1}\mathbf{T}\left(\mathbf{D}_D^{JJ}\right)^{-1}\mathbf{D}_D^{JI} & \mathbf{S}^{-1} \end{bmatrix}
\end{aligned} \tag{26}$$

where

$$\mathbf{S} = \mathbf{T}\left(\mathbf{D}_D^{JJ}\right)^{-1}\mathbf{T}^T$$

$$\mathbf{Q} = \left(\mathbf{D}_D^{JJ}\right)^{-1}\mathbf{T}^T\mathbf{S}^{-1}\mathbf{T}\left(\mathbf{D}_D^{JJ}\right)^{-1} - \left(\mathbf{D}_D^{JJ}\right)^{-1}$$

The state-space model in Eq. (21) with matrices defined in Eq. (26) will be referred to as the coupled-substructure state-space model. This model describes the dynamics of the substructures when their interface compatibility and equilibrium conditions are enforced. Therefore, it has the exact input–output transfer function and can be considered as a state-space model for the assembled structure. However, this state-space model is not a minimal-order model for the assembled structure. For every pair of interface degrees of freedom that are connected, one of them should drop out of the assembled structure. Consequently, for every pair of connected interface degrees of freedom, two state variables should be eliminated from the coupled-substructure model. Elimination of these extra state variables can be accomplished by using a minimal realization algorithm.

For the two-substructure structure shown in Fig. 2, let the state, input, and output vectors of the coupled-substructure system be defined by

$$\mathbf{x} = \begin{Bmatrix} x_\alpha \\ x_\beta \end{Bmatrix}, \qquad \bar{\mathbf{u}} = \begin{Bmatrix} \bar{u}_\alpha^I \\ \bar{u}_\beta^I \\ \bar{u}^J \end{Bmatrix}, \qquad \bar{\mathbf{y}} = \begin{Bmatrix} \bar{y}_\alpha^I \\ \bar{y}_\beta^I \\ \bar{y}^J \end{Bmatrix}$$

Then, by using Eq. (26) it is easy to show that the coupled-substructure state-space model for the two-substructure structure is described by the following matrices where $S = (D_\alpha^{JJ} + D_\beta^{JJ})^{-1}$:

$$\begin{aligned}
(\bar{\mathbf{A}}, \bar{\mathbf{B}}, \bar{\mathbf{C}}, \bar{\mathbf{D}}) = \Bigg(& \begin{bmatrix} A_\alpha - B_\alpha^J S C_\alpha^J & B_\alpha^J S C_\beta^J \\ B_\beta^J S C_\alpha^J & A_\beta - B_\beta^J S C_\beta^J \end{bmatrix} \\
& \begin{bmatrix} B_\alpha^I - B_\alpha^J S D_\alpha^{JI} & B_\alpha^J S D_\beta^{JI} & B_\alpha^J S D_\beta^{JJ} \\ B_\beta^J S D_\alpha^{JI} & B_\beta^I - B_\beta^J S D_\beta^{JI} & B_\beta^J S D_\alpha^{JJ} \end{bmatrix} \\
& \begin{bmatrix} C_\alpha^I - D_\alpha^{IJ} S C_\alpha^J & D_\alpha^{IJ} S C_\beta^J \\ D_\beta^{IJ} S C_\alpha^J & C_\beta^I - D_\beta^{IJ} S C_\beta^J \\ D_\beta^{JJ} S C_\alpha^J & D_\alpha^{JJ} S C_\beta^J \end{bmatrix} \\
& \begin{bmatrix} D_\alpha^{II} - D_\alpha^{IJ} S D_\alpha^{JI} & D_\alpha^{IJ} S D_\beta^{JI} & D_\alpha^{IJ} S D_\beta^{JJ} \\ D_\beta^{IJ} S D_\alpha^{JI} & D_\beta^{II} - D_\beta^{IJ} S D_\beta^{JI} & D_\beta^{IJ} S D_\alpha^{JJ} \\ D_\beta^{JJ} S D_\alpha^{JI} & D_\alpha^{JJ} S D_\beta^{JI} & D_\alpha^{JJ} S D_\beta^{JJ} \end{bmatrix} \Bigg)
\end{aligned} \tag{27}$$

In the preceding derivations, we made an assumption that D_D^{JJ} is invertible [see Eq. (26)], which implies that D_i^{JJ}, $i = \alpha, \beta, \gamma, \ldots$, are invertible. Such an assumption is valid when the substructure interface outputs are accelerations. Let M_α denote the mass matrix of α-substructure. It can be shown that if the interface outputs are accelerations, then $D_\alpha^{JJ} = (M_\alpha^{-1})^{JJ}$ (i.e. the JJ portion of M_α^{-1}), which is invertible because the mass matrix of a real structure is positive definite. When the interface outputs of α-substructure are velocities, the direct force input term is zero, i.e., $D_\alpha^{JJ} = 0$. In this case, the interface input–output transfer function of α-substructure is given by

$$H_\alpha^{JJ} = C_\alpha^J(sI - A_\alpha)^{-1}B_\alpha^J \tag{28}$$

Recall that multiplication by s in the Laplace domain is equivalent to differentiation with respect to time in the time domain. We can multiply the preceding velocity interface output transfer function by s to obtain an acceleration interface output transfer function. Using matrix algebra, we obtain

$$\begin{aligned}
sH_\alpha^{JJ} &= sC_\alpha^J(sI - A_\alpha)^{-1}B_\alpha^J \\
&= C_\alpha^J(sI - A_\alpha)^{-1}A_\alpha B_\alpha^J + C_\alpha^J B_\alpha^J
\end{aligned} \tag{29}$$

Theoretically, the direct force input term $C_\alpha^J B_\alpha^J$ in the preceding expression is equal to $(M_\alpha^{-1})^{JJ}$. Therefore, synthesis of substructure state-space models with velocity interface outputs can be achieved by using $C_\alpha B_\alpha^J$ to replace D_α^{JJ}, $A_\alpha B_\alpha^J$ to replace B_α^J, and so on, in the assembling process. Synthesis of substructure state-space models with displacement interface outputs can be done in a similar fashion.

Synthesis of Substructure Markov Parameters

Synthesis formulas for substructure Markov parameters can be derived by using the assembled transfer function expressions in Eq. (10). First, let us define Markov parameters. The transfer function of a continuous-time system (A, B, C, D) can be expressed in the following series form:

$$\begin{aligned}
H(s) &= C(sI - A)^{-1}B + D \\
&= D + \frac{CB}{s} + \frac{CAB}{s^2} + \frac{CA^2B}{s^3} + \cdots \\
&= \sum_{i=0}^{\infty} P_i s^{-i}
\end{aligned} \tag{30}$$

where

$$P_0 = D, \quad P_i = CA^{i-1}B, \quad \text{for} \quad i = 1, 2, \ldots, \infty \tag{31}$$

The matrices, various P_i in the preceding series are called the ith Markov parameter of the system. Before moving on to establish a procedure for assembling substructure Markov parameters, it is

necessary to show how to determine Markov parameters for interconnected systems.

Use the notation $\mathrm{MP}(H) = P_i$ to indicate that the Markov parameters of the transfer function H are P_i. Let $\mathrm{MP}(H_a) = P_{ai}$ and $\mathrm{MP}(H_b) = P_{bi}$. Obviously, for parallel connection,

$$\mathrm{MP}(H_a + H_b) = P_{ai} + P_{bi} \tag{32}$$

For series connection,

$$H_a(s)H_b(s) = \left(P_{a0} + \frac{P_{a1}}{s} + \frac{P_{a2}}{s^2} + \cdots\right)\left(P_{b0} + \frac{P_{b1}}{s} + \frac{P_{b2}}{s^2} + \cdots\right)$$

Carrying out the multiplication, it can be shown that

$$\mathrm{MP}(H_aH_b) = \sum_{j=0}^{i} P_{aj}P_{b,i-j} \tag{33}$$

which is a convolution summation formula. Use the operator $*$ to denote convolution summation. Then, Eq. (33) also can be expressed as

$$\mathrm{MP}(H_aH_b) = P_{ai} * P_{bi} \tag{34}$$

For an inverted transfer function H^{-1}, let its Markov parameters be denoted by $\tilde{P}_i$. Then, by using the identity $H(s)H(s)^{-1} = I$, we obtain

$$I = \left(P_0 + \frac{P_1}{s} + \frac{P_2}{s^2} + \cdots\right)\left(\tilde{P}_0 + \frac{\tilde{P}_1}{s} + \frac{\tilde{P}_2}{s^2} + \cdots\right)$$

which yields

$$\tilde{P}_0P_0 = I, \qquad \tilde{P}_1P_0 + \tilde{P}_0P_1 = 0$$
$$\tilde{P}_2P_0 + \tilde{P}_1P_1 + \tilde{P}_0P_2 = 0, \ldots, \text{etc.}$$

The preceding identities indicate that $\tilde{P}_i$ can be calculated by

$$\tilde{P}_0 = P_0^{-1}$$
$$\tilde{P}_i = -\left(\sum_{j=0}^{i-1} \tilde{P}_jP_{i-j}\right)\tilde{P}_0, \qquad i = 1, 2, \ldots, \infty \tag{35}$$

in which the parenthesized term is a convolution summation. We will call $\tilde{P}_i$ the convolution inverse of P_i. Note that for Eq. (35) to be valid, the first Markov parameter P_0, which is equal to the direct force-input term D, must be invertible. If $P_0 = 0$, then the shifted Markov parameter sequence $P_1, P_2, P_3, \ldots$ (which are the Markov parameters of sH) should be used to determine the convolution inverse, provided that P_1 is invertible. This follows from $H^{-1} = s(sH)^{-1}$.

Markov parameters also can be partitioned. Let the Markov parameters of α-substructure and β-substructure be partitioned according to the partitions of substructure transfer functions in Eqs. (1) and (2) as

$$P_{\alpha i} = \begin{bmatrix} P_{\alpha i}^{II} & P_{\alpha i}^{IJ} \\ P_{\alpha i}^{JI} & P_{\alpha i}^{JJ} \end{bmatrix}, \qquad P_{\beta i} = \begin{bmatrix} P_{\beta i}^{II} & P_{\beta i}^{IJ} \\ P_{\beta i}^{JI} & P_{\beta i}^{JJ} \end{bmatrix} \tag{36}$$

Then, it can be shown that

$$\mathrm{MP}\left(H_\alpha^{II}\right) = P_{\alpha i}^{II}, \qquad \mathrm{MP}\left(H_\alpha^{IJ}\right) = P_{\alpha i}^{IJ}, \ldots$$
$$\mathrm{MP}\left(H_\beta^{II}\right) = P_{\beta i}^{II}, \qquad \mathrm{MP}\left(H_\beta^{IJ}\right) = P_{\beta i}^{IJ}, \ldots \tag{37}$$

and so on.

With the preceding definitions and establishments, the procedure for assembling substructure Markov parameters can be derived in a straightforward manner. Take the two-substructure structure in Fig. 2 for example. From the assembled transfer function expressions in Eq. (10), it is easy to see that the Markov parameters for the assembled structure are given by

$$\tilde{P}_i = \begin{bmatrix} P_{\alpha i}^{II} - P_{\alpha i}^{IJ} * R * P_{\alpha i}^{JI} & P_{\alpha i}^{IJ} * R * P_{\beta i}^{JI} & P_{\alpha i}^{IJ} * R * P_{\beta i}^{JJ} \\ P_{\beta i}^{IJ} * R * P_{\alpha i}^{JI} & P_{\beta i}^{II} - P_{\beta i}^{IJ} * R * P_{\beta i}^{JI} & P_{\beta i}^{IJ} * R * P_{\alpha i}^{JJ} \\ P_{\beta i}^{JJ} * R * P_{\alpha i}^{JI} & P_{\alpha i}^{JJ} * R * P_{\beta i}^{JI} & P_{\alpha i}^{JJ} * R * P_{\beta i}^{JJ} \end{bmatrix} \tag{38}$$

where R is the convolution inverse of $(P_{\alpha i}^{JJ} + P_{\beta i}^{JJ})$. For multiple substructures case, the synthesis formulas can be derived similarly by using Eq. (17).

Testing Difficulties and Possible Solutions

In actual testing situations, the requirement of a collocated actuator/sensor at every interface degree of freedom may present difficulty. The suspension system used to support substructures also changes the actual dynamics of the substructures to be identified. In the following, some testing difficulties will be discussed along with possible solution approaches proposed.

Mass-Loaded Interface Approach

First, we will show that by adding mass to the substructure interface, the requirement of placing collocated actuators and sensors at the interface can be avoided. Consider the substructure shown in Fig. 3a, whose interface is loaded with a mass m. The input u^I is applied to an interior point. Our objective is to determine the interface input–output transfer function for the original substructure (the one without the added mass) from the test data of the mass-loaded substructure.

The interface output Y^J of the mass-loaded substructure due to the interior input U^I can be represented by

$$Y^J = H_m^{JI}U^I \tag{39}$$

where subscript m is used to indicate that the transfer function data are measured when the substructure's interface is loaded with a mass m. Figure 3b shows that Y^J also can be interpreted as the output response of the original substructure due to U^I and, in addition, an inertia force U^J applied at the interface. That is,

$$Y^J = H^{JI}U^I + H^{JJ}U^J \tag{40}$$

where H^{JI} and H^{JJ} represent transfer functions of the original substructure, and

$$U^J = -m\,Y^J \tag{41}$$

is the inertia force induced by the added mass m. Here we have

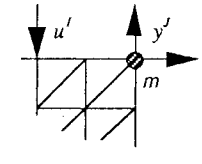

a) Mass-loaded

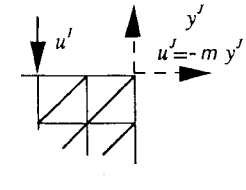

b) Equivalent

Fig. 3 Comparison of identified poles and exact poles of the assembled system.

assumed that output Y^J is acceleration. Combining Eqs. (39–41), we obtain

$$H_m^{JI} = H^{JI} - H^{JJ} m H_m^{JI} \tag{42}$$

Or,

$$H_m^{JI} = [H^{JI} \quad H^{JJ}] \begin{bmatrix} I \\ -mH_m^{JI} \end{bmatrix} \tag{43}$$

The preceding equation is underdetermined for the solutions of H^{JI} and H^{JJ}. We can perform several tests by using different masses, $m_1, m_2, \ldots$, and sum up the test results into one equation as

$$\begin{bmatrix} H_{m_1}^{JI} & H_{m_2}^{JI} & \cdots \end{bmatrix} = [H^{JI} \quad H^{JJ}] \begin{bmatrix} I & I & \cdots \\ -m_1 H_{m_1}^{JI} & -m_2 H_{m_2}^{JI} & \cdots \end{bmatrix} \tag{44}$$

Although theoretically the solutions of H^{JI} and H^{JJ} are unique, the preceding equation is generally overdetermined because of the noises in the test data. A least-square solution method can be used to solve Eq. (44).

The preceding derivations show that by adding masses to the interfaces of substructures, the information that is needed for performing substructure coupling, i.e., H^{JJ}, can be obtained without the need of placing collocated actuators and sensors at the interface. Adding masses to a substructure also lowers the natural frequencies of that substructure. For substructures that are stiff and have high natural frequencies, this effect at times can make the testing easier to do.

Spring-Supported Boundary Approach

After a structure is decomposed into several substructures, most of the substructures will be free of any constraint. A free substructure must be supported by a suspension system, e.g., hung by bungee cords or supported by air bags, in order to be tested on the ground. Using a suspension system to support substructures always affects the accuracy of the test data. Here we will present a procedure to determine transfer functions for a free substructure from the test data acquired while the substructure's boundary is supported by springs.

Let the input–output transfer function relation of the spring-supported substructure shown in Fig. 4a be described by

$$\begin{Bmatrix} Y^I \\ Y^J \end{Bmatrix} = \begin{bmatrix} H_k^{II} \\ H_k^{JI} \end{bmatrix} U^I \tag{45}$$

Subscript k is used to indicate that the substructure boundary is supported by a spring with spring constant k. Superscript J is borrowed from previous usage to denote boundary degrees of freedom, which also can be interface degrees of freedom. Figure 4b shows that the output responses of the spring-supported substructure due to U^I also can be interpreted as the output responses of the original substructure due to U^I and, at the same time, a spring force U^J applied at the boundary. That is,

$$\begin{Bmatrix} Y^I \\ Y^J \end{Bmatrix} = \begin{bmatrix} H^{II} & H^{IJ} \\ H^{JI} & H^{JJ} \end{bmatrix} \begin{Bmatrix} U^I \\ U^J \end{Bmatrix} \tag{46}$$

where

$$U^J = -k Y^J / (j\omega)^2 \tag{47}$$

is the spring force. Combining Eqs. (45–47), we obtain

$$\begin{bmatrix} H_k^{II} \\ H_k^{JI} \end{bmatrix} = \begin{bmatrix} H^{II} \\ H^{JI} \end{bmatrix} - \begin{bmatrix} H^{IJ} \\ H^{JJ} \end{bmatrix} k H_k^{JI} / (j\omega)^2 \tag{48}$$

Or,

$$\begin{bmatrix} H_k^{II} \\ H_k^{JI} \end{bmatrix} = \begin{bmatrix} H^{II} & H^{IJ} \\ H^{JI} & H^{JJ} \end{bmatrix} \begin{bmatrix} I \\ -k H_k^{JI} / (j\omega)^2 \end{bmatrix} \tag{49}$$

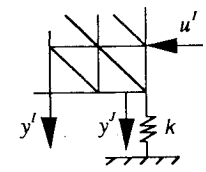

a) Spring-supported

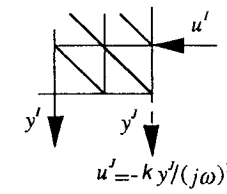

b) Equivalent

Fig. 4 Substructure with spring-supported boundary.

The preceding equation is undetermined. One can perform several tests by using different springs and summarize the test data into one equation as

$$\begin{bmatrix} H_{k_1}^{II} & H_{k_2}^{II} & \cdots \\ H_{k_1}^{JI} & H_{k_2}^{JI} & \cdots \end{bmatrix} = \begin{bmatrix} H^{II} & H^{IJ} \\ H^{JI} & H^{JJ} \end{bmatrix} \begin{bmatrix} I & I & \cdots \\ -k_1 H_{k_1}^{JI} / (j\omega)^2 & -k_2 H_{k_2}^{JI} / (j\omega)^2 & \cdots \end{bmatrix} \tag{50}$$

Then, by using a least-square approach, the transfer functions for the free substructure can be solved.

In actual experiments, metal rods can be used as springs to support free substructures. The effective spring constants in the axial and transverse directions can be determined by using engineering beam theory or by experiment. An even more effective approach would be to measure the spring forces directly by placing force gauges at the spring attachment points.

Measurement and Excitation of Rotational Degrees of Freedom

The most difficult testing task is probably the measurement and excitation of rotational degrees of freedom. The substructure synthesis methods presented in this paper are exact methods only if all the substructure interface input–output transfer function data are measured. All the effective interface degrees of freedom, which include not only translational degrees of freedom but also rotational degrees of freedom, must be excited and measured. Unfortunately,

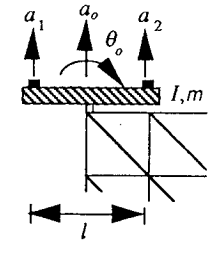

a)

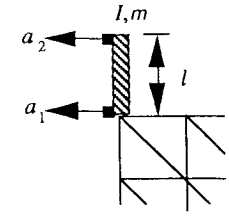

b)

Fig. 5 Testing setups for the measurement of rotational degrees-of-freedom.

measuring or exciting rotational degrees-of-freedom has never been an easy task in practical situations.

Reference 2 has a brief discussion on the measurement of rotational degrees of freedom. It is proposed that a pair of matched conventional accelerometers can be placed a short distance apart on a fixture attached to the structure as shown in Fig. 5a. The responses a_0 and θ_0 at the attachment point can be calculated by taking the mean and difference of the two accelerometer outputs a_1 and a_2 as

$$a_0 = (a_1 + a_2)/2$$
$$\theta_0 = (a_1 - a_2)/l \tag{51}$$

Therefore, it is possible to measure interface rotational degrees of freedom to acceptable accuracy if the experiment is done carefully. Another configuration of testing setup is shown in Fig. 5b. The attached fixture must be very rigid compared with the substructures in order for the proposed approach to be successful. There also exist commercial sensors that can be used to measure rotational degrees of freedom.

Applying moment-type excitations (or torques) to the interfaces of substructures is even harder than measuring rotational responses. Fortunately, instead of using torque wheels to apply torques externally, we can attach a rigid fixture with substantial moment-inertia to a substructure's interface and use it to provide inertia-induced excitations to the interface rotational degrees of freedom. Then, a moment-inertia-loaded interface approach, which is similar to the mass-loaded interface approach described previously, can be employed to determine the interface input–output transfer function data for the substructure. Of course, a great deal of engineering and artistic efforts may be required in setting up a good experiment, especially for three-dimensional structures of which every interface node has three translational degrees of freedom and three rotational degrees of freedom.

Effect of Discrete-Time Data Sampling

All the derivations in this paper are based on continuous-time models of flexible structure systems. However, in actual situations the input–output time history data acquired in experiments are sampled time history data measured at a sequence of time points. Discrete-time data sampling leads to discrete-time substructure transfer function data, discrete-time substructure state-space models, and discrete-time substructure Markov parameters, as opposed to their continuous-time counterparts.

It should be pointed out that the substructure synthesis methods proposed here are only valid for assembling continuous-time substructure models. Applying the proposed methods to assemble discrete-time substructure models does not yield an exact discrete-time model for the assembled structure. Let us use the interconnection of two transfer functions for explanation. The most frequently used data sampling method in experiments is the so-called zero-order-hold (ZOH) approach. The ZOH conversion formula between the discrete-time transfer function and the continuous-time transfer function is given by

$$H(z) = \frac{z-1}{z}\mathcal{Z}\left\{\frac{H(s)}{s}\right\} \tag{52}$$

where $\mathcal{Z}\{\ \}$ denotes the z transform. Let $H_1(s)$ and $H_2(s)$ be the continuous-time transfer functions of two systems and let $H_1(z)$ and $H_2(z)$ be their ZOH discrete-time transfer functions. For parallel connection, $H_1(z)+H_2(z)$ is equal to the ZOH discrete transform of $H_1(s) + H_2(s)$. However, for series connection, $H_1(z)H_2(z)$ is not equal to the ZOH discrete transform of $H_1(s)H_2(s)$. Likewise, $H_1^{-1}(z)$ is not the ZOH discrete transform of $H_1^{-1}(s)$. The assembled structure transfer functions in Eq. (10) involve addition, multiplication, and inversion of substructure transfer functions. From the foregoing discussions, it is clear that simply replacing the s variable in Eq. (10) by the z variable does not yield synthesis formulas for assembling discrete-time substructure transfer functions. For the same reason, Eq. (26) is not valid for assembling ZOH discrete-time substructure state-space models and Eq. (38) is not valid for assembling ZOH discrete-time substructure Markov parameters (also called the pulse response data).

Unfortunately, the results of system identification are discrete-time models because the test data are discrete by nature. The identified discrete-time substructure models must be converted to the continuous-time domain before performing synthesis. Accuracy of the continuous-time models thus obtained largely depends on the size of the sampling period. One should set the sampling period to be sufficiently small so that the test data–derived substructure models, after being converted to the continuous-time domain, have acceptable accuracy for substructure synthesis purpose.

Numerical Example

The substructure synthesis methods proposed in this paper have not been applied to real experimental data yet. A numerical simulation example is included here for demonstration. Consider the mass-spring-damper system shown in Fig. 6. The two substructures α and β are to be connected by using the massless rigid links on mass 4 and mass 5. The outputs of the α-substructure are y_1 = displacement and y_2 = acceleration, and the outputs of the β-substructure are y_3 = acceleration and y_4 = displacement. All of the inputs are forces.

System identification at the substructure level was done based on the substructures' input and output time history data by using the system/observer/controller identification toolbox (SOCIT).[9] The input forces are assumed to be normally distributed random inputs with mean 0 and variance 1. The substructures' outputs are sampled at 1024 time points with sampling period 0.1, which is about one-eighth of the shortest natural period of the assembled system. For the noise-free case, the substructure state-space model synthesis procedure yields an exact model for the assembled system. Therefore, the results of noise-free system identification are not shown here. To simulate noise situations, a normally distributed random noise with a 3% noise-to-signal ratio is added to each output data. Results of substructure system identification with output noises are listed in Tables 1 and 2, in which the substructure state-space models are presented in modal coordinates. The substructure system matrices A_α and A_β are formed by the identified system poles and are in a block-diagonal form (i.e, in a real, block-diagonal modal representation). From Table 2, it is seen that the two poles associated with the rigid-body mode of the β-substructure are not very accurately identified because of the noises.

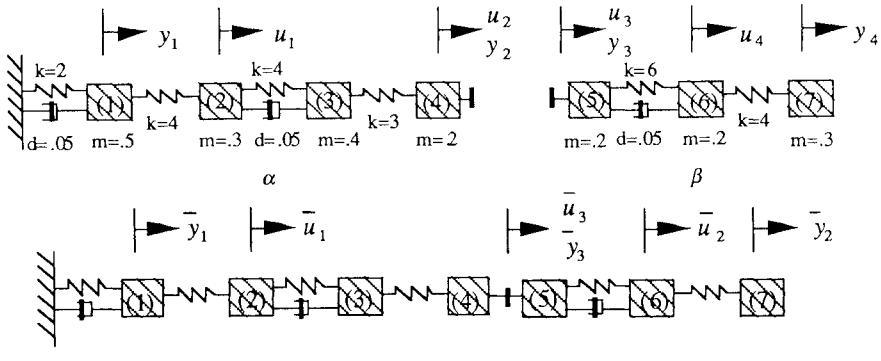

Fig. 6 Mass-spring-damper example.

Table 1 Identified model of α-substructure[a]

Identified poles	Exact poles
$-0.0097 \pm j1.0222$	$-0.0097 \pm j1.0222$
$-0.0504 \pm j2.9535$	$-0.0505 \pm j2.9531$
$-0.0068 \pm j4.7604$	$-0.0076 \pm j4.7603$
$-0.1345 \pm j6.2176$	$-0.1281 \pm j6.2219$

$$B_\alpha, C_\alpha, D_\alpha =$$

$$\begin{bmatrix} 0.3580 & 0.4834 \\ 0.3056 & 0.4006 \\ 0.1106 & -0.2770 \\ -0.2928 & 0.8109 \\ 0.3268 & -0.6816 \\ 0.1114 & -0.2519 \\ -0.3064 & -0.1575 \\ -0.9527 & -0.3089 \end{bmatrix}, \quad \begin{bmatrix} -0.6518 & 1.1578 \\ 0.7745 & -1.4349 \\ 0.4651 & 4.4387 \\ 0.1588 & 1.3728 \\ 0.0750 & -5.1024 \\ -0.2304 & 14.1133 \\ -0.0856 & -4.2608 \\ 0.0329 & 1.4346 \end{bmatrix}^T$$

$$\begin{bmatrix} -0.0009 & -0.0006 \\ 0.0074 & 5.0081 \end{bmatrix}$$

[a]Data with 3% random noise.

Table 2 Identified model of β-substructure[a]

Identified poles	Exact poles
0.0209	0
−0.0237	0
$-0.0226 \pm j4.3342$	$-0.0204 \pm j4.3340$
$-0.2301 \pm j8.6286$	$-0.2296 \pm j8.6300$

$$B_\beta, C_\beta, D_\beta =$$

$$\begin{bmatrix} -3.1906 & -3.1379 \\ -3.6572 & -3.5941 \\ 0.5625 & 0.2073 \\ 0.6265 & 0.2392 \\ -0.2063 & 0.2798 \\ 0.6719 & -1.0086 \end{bmatrix}, \quad \begin{bmatrix} -0.0277 & -10.1858 \\ 0.0208 & 8.8918 \\ 8.1178 & 0.3938 \\ -7.2204 & -0.3514 \\ 17.9099 & -0.0762 \\ 3.5349 & -0.0272 \end{bmatrix}^T$$

$$\begin{bmatrix} 5.0223 & 0.0148 \\ 0.0006 & 0.0004 \end{bmatrix}$$

[a]Data with 3% random noise.

Table 3 Comparison of identified poles and exact poles of the assembled system

Identified poles	Exact poles
$-0.1705 \pm j8.1084$	$-0.1699 \pm j8.1084$
$-0.1404 \pm j6.1574$	$-0.1293 \pm j6.1532$
$-0.0124 \pm j4.5636$	$-0.0131 \pm j4.5616$
$-0.0378 \pm j3.5375$	$-0.0424 \pm j3.5173$
$-0.0236 \pm j2.1577$	$-0.0245 \pm j2.1454$
$-0.0043 \pm j0.7372$	$-0.0041 \pm j0.7361$

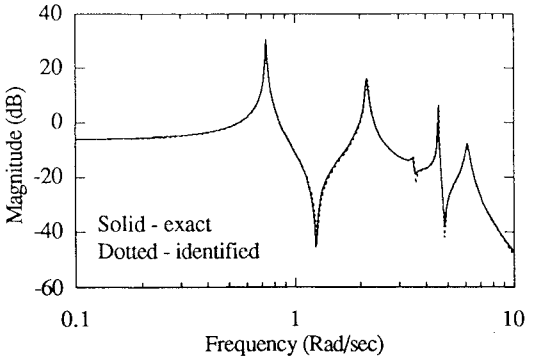

Fig. 7 Comparison of transfer function $\bar{H}_{11}$ of the identified model and the exact model.

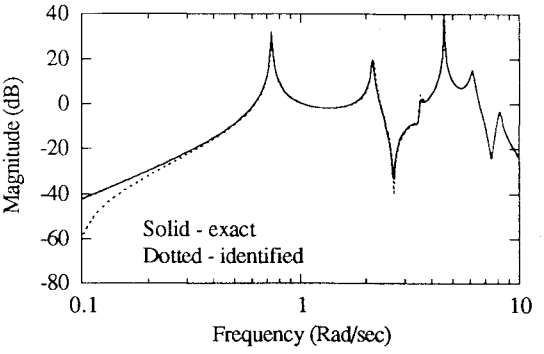

Fig. 8 Comparison of transfer function $\bar{H}_{31}$ of the identified model and the exact model.

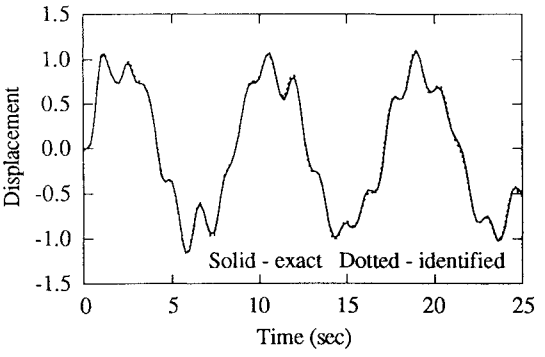

Fig. 9 Comparison of impulse responses of the identified model and the exact model ($\bar{y}_2$ due to $\bar{u}_3$).

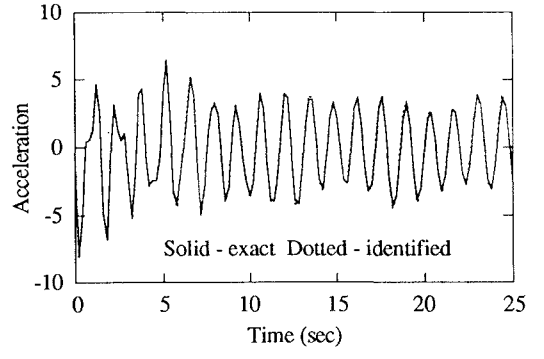

Fig. 10 Comparison of impulse responses of the identified model and the exact model ($\bar{y}_3$ due to $\bar{u}_3$).

The two identified substructure state-space models are assembled by using Eq. (27). Then, minimal realization is performed to the coupled-substructure state-space model to obtain a minimal-order model for the assembled system. Table 3 compares the poles of the identified model with the exact poles of the assembled system. It is seen that the system poles are identified with high accuracy. Figures 7 through 10 compare some transfer functions and impulse responses of the identified model and the exact model of the assembled system. It is evident that the system has been accurately identified by the proposed substructure system identification method.

Concluding Remarks

The possibility of performing system identification at the substructure level and then using a substructure synthesis concept to assemble the substructure models has been investigated in this paper. It is found that coupling of substructure test data and substructure state-space models can be accomplished by enforcing compatibility and equilibrium conditions at the interface. Procedures for assembling substructure transfer function data, substructure state-space models, and substructure Markov parameters have been developed. We also have looked into some potential difficulties during the actual

test and proposed possible solution approaches. It is found that to produce exact substructure coupling, all the substructure interface input–output transfer functions must be measured, which implies the requirement of placing collocated actuators and sensors at all the interface degrees of freedom. However, this requirement can be avoided by employing a mass-loaded interface approach, in which lumped masses are added to the substructures' interfaces to provide the required interface excitations. For the testing and system identification of free substructures, a spring-supported boundary approach is proposed to determine the data for the free substructures from the test data of the spring-supported substructures. As to the measurement and excitation of the interface rotational degrees of freedom, we propose using a dual-accelerometer testing setup and a moment-inertia-loaded interface approach. It is also pointed out that the proposed substructure synthesis methods are valid only for assembling continuous-time substructure models. The sampling time of the test data must be set small enough to obtain accurate results. A numerical example is provided to show the efficacy of the proposed methods.

Acknowledgment

This research work was done while the first author held a National Research Council Research Associateship at the NASA Langley Research Center.

References

[1]Craig, R. R., Jr., "A Review of Time-Domain and Frequency-Domain Component Mode Synthesis Methods," *International Journal of Analytical and Experimental Modal Analysis,* Vol. 2, No. 2, 1987, pp. 59–72.

[2]Ewins, D. J., *Modal Testing: Theory and Practice,* Research Studies Press, Letchworth, Hertfordshire, England, UK, 1984.

[3]Anon., *User Manual for Modal Analysis 9.0,* SDRC/CAE International, 1985.

[4]Ho, B. L., and Kalman, R. E., "Effective Construction of Linear State Variable Models from Input/Output Data," *Proceedings of the 3rd Annual Allerton Conference on Circuits and Systems Theory* (Monticello, IL), 1965.

[5]Juang, J. N., and Pappa, R. S., "An Eigensystem Realization Algorithm for Modal Parameter Identification and Modal Reduction," *Journal of Guidance, Control, and Dynamics,* Vol. 8, No. 5, 1985, pp. 620–627.

[6]Juang, J. N., "Mathematical Correlation of Modal-Parameter-Identification Methods Via System Realization Theory," *International Journal of Analytical and Experimental Modal Analysis,* Vol. 2, No. 1, 1987, pp. 1–18.

[7]Klosterman, A., "On the Experimental Determination and Use of Modal Representations of Dynamic Characteristics," Ph.D. Dissertation, Dept. of Mechanics and Industrial Engineering, Univ. of Cincinnati, Cincinnati, OH, 1971.

[8]Moser, A. L., "An Experimental Investigation of Modeling and Optimal Control of Modified Space Structures," Ph.D. Dissertation, Applied Mechanics Dept., California Inst. of Technology, Pasadena, CA, 1992.

[9]Juang, J. N., Horta, L. G., and Phan, M., "System/Observer/Controller Identification Toolbox," NASA TM-107566, Feb. 1992.